

STUDY THE EFFECT OF CO₂ MAG WELDING PROCESS PARAMETERS ON THE HEAT INPUT AND JOINT GEOMETRY DIMENSIONS USING EXPERIMENTAL AND COMPUTATIONAL METHODS

Samir Ali Amin Alrabii¹, Salah Sabeeh Abed-Alkarem²

¹ Assistant Professor, Mechanical Engineering Department, University of Technology.

² Lecturer, Department of Machines and Agricultural Equipment, University of Baghdad.

E-mail: arabiee2002@yahoo.com¹, dr.salah2007@yahoo.com²

(Received: 20/1/2014; Accepted: 14/4/2014)

ABSTRACT:-In this paper, predicted models for heat input and joint geometry dimensions after CO₂-MAG welding process have been developed. Before welding, steel specimens were first prepared and then butt welded using electrode wire melted and supplied into the molten pool by applying heat input continuously. Weld bead dimensions were first measured, and then the results were analyzed to check the adequacy of the models by Response Surface Method using DOE technique. These models were found capable of predicting the optimum performance dimensions required for the joint geometry in terms of weld bead width, reinforcement height and penetration. The obtained results indicated that the heat input depends on voltage, wire feed speed and gas flow rate, while for the weld bead dimensions; the gas flow rate has less effect. A comparison between the experimental and predicted results was made, and a good agreement was found between them.

Keywords: Low Carbon Steel, CO₂-MAG Process, Heat input, Joint Geometry, Modeling, Experimental and Computational Methods, Optimization.

1. INTRODUCTION

CO₂-MAG is an arc welding process where heat is generated for arc between the workpiece and a consumable metal electrode with an externally supplied gaseous shield of gas either inert, such as CO₂. It is a versatile process, gives very little loss of alloying elements and can be operated as semi as well as fully automated. A bare solid wire called electrode is continuously fed to the weld zone, it becomes filler metal as it is consumed. Electrical energy is supplied from the welding generator for melting wire and workpiece to be welded. The weld is made by falling successive drops on the weld puddle. The arc and the molten puddle are protected from contamination by the atmosphere (i.e., oxygen and

nitrogen) with an externally supplied gaseous shield of gas, such as CO₂ which is a reactive gas and is about 1.5 times heavier than air ⁽¹⁾.

CO₂ gas is an odorless, colorless gas with a slightly pungent, acid taste and slightly toxic. Differing from other reactive gases such as oxygen, CO₂ can be used alone for GMAW shielding gas applications. Pure CO₂ is the cheapest of the shielding gases and can be used as a shield for welding steel up to 0.4% C and low-alloy steel. All the major commercial metals can be welded by the process CO₂-MAG, including carbon steels, stainless steels, aluminum, copper, titanium, Because there is some dissociation of the CO₂ in the arc resulting in carbon monoxide and oxygen being formed, the filler wire is triple deoxidized to prevent porosity, and this adds somewhat to its cost and results in some small areas of slag being present in the finished weld ⁽²⁾.

Gas flow rate can greatly affect the quality of the weld, since too low a flow rate gives inadequate gas shielding and leads to the inclusion of oxides and nitrides, while too high flow rate can introduce a turbulent flow of the CO₂ which occurs at a lower rate than with argon ⁽³⁾. This affects the efficiency of the shield and leads to a porosity in the weld. Also, gas flow rate, which can range from a few cubic feet per hour (cfh) to more than 60 cfh, depends on the current developed, the torch size, the shielding gas composition and the surrounding environment (drafts, etc.). In general, a higher current will require a larger torch and higher flow rates. In addition, gas density, or the weight of the gas relative to air, has a major influence on the minimum flow rate required to effectively shield the weld ⁽³⁾.

Welding with the recommended heat input results in good mechanical properties in the heat affected zone (HAZ). The heat supplied by the welding process affects the mechanical properties of the welded joint. Heat input can be referred to as "the electrical energy supplied by the welding arc to the workpiece. The most important characteristic of heat input is that it governs the cooling rates in welds and thereby affects the microstructure of the weld metal and the heat affected zone. A change in microstructure directly affects the mechanical properties of welds. Therefore, the control of heat input is very important in arc welding in terms of quality control ⁽⁴⁾.

Quality of the welded joint in CO₂-MAG welding process depends on number of parameters, like type and thickness of base metal, design type, welding position, etc., but the proper selection of welding parameters is also very important. Due to that, the weld bead geometry in CO₂-MAG welding process and heat input with regard to weld voltage, wire feeding speed and gas flow rate were experimentally investigated in the present work, since the proper selection of gas flow and heat input will provide a weld joint with satisfactory geometrical characteristics ⁽⁵⁾.

A large amount of research works have been carried out to find out the most suitable combination of input process parameters for a desired output using different welding processes and various computer software as tools for modeling and optimization the weld bead geometry, such as Taguchi ⁽⁶⁾, Artificial neural networks (ANN) ⁽⁷⁾, and Response surface methodology (RSM) ⁽⁸⁾. Das et al. ⁽⁹⁾ studied the effect of arc voltage, current and welding speed on the weld joint geometry, while Shoeb et al. ⁽¹⁰⁾ considered also the influence of gas flow rate. In addition, Patel and Patel ⁽¹¹⁾ investigated also the wire diameter and wire feed rate during CO₂-MAG welding process. But, there is a little work about modeling and computational optimization of the closed butt weld bead geometry by using Design of Experiment (DOE) with (RSM) technique to predict mathematical models that can be used to obtain the optimum responses for any given input parameters. Therefore, the aim of this paper is to study the influence of main welding parameters (voltage, wire feeding speed and gas flow rate) on the heat input and final weld pool geometry during CO₂-MAG welding using DOE and RSM method.

2. EXPERIMENTAL PROCEDURES

2.1 Material and Specimens Preparation

The material used in the present work is low carbon steel (LCS) plate with 5 mm thickness in the hot rolled condition. This material was chemically analyzed in State Company for Inspection and Engineering Rehabilitation (SIER) in Baghdad, and its chemical composition is given in Table (1), showing that the experimental material conforms to the standard low carbon steel type AISI 1010 ⁽¹²⁾. The plate was cut to provide specimens with size 50 mm× 25 mm×5 mm to be welded in a closed Butt weld joint design by CO₂-MAG process. Specimens from the as-received material were tensile tested according to ASTM E8 in Strength Laboratory / University of Technology-Baghdad, and the results are given in Table (2).The results in this table represent the average of three readings (three samples).

2.2 Selection of Welding Parameters

Despite the use of CO₂- MAG welding process is influenced by number of Parameters, three of them were only selected in this investigation: voltage, wire feeding speed and gas flow rate in two levels (input parameters), as shown in Table (3). These parameters were chosen according to the capacity of CO₂- MAG welding machine and practical experience of the welder skill.

2.3 Welding Procedure

Twenty specimens were welded by CO₂-MAG process at different values of voltage, wire feeding speed and gas flow rate according to design matrix established by Design of

Experiment Version 8 Software as given in Table (4). The experiments were performed in random manner to avoid any systematic error. The welding machine type ‘INVERTER CO₂ MAG - BEAM-350’ was used for welding the specimens in Korea-Iraq Vocational Training Center in Baghdad, with wire a filler type ‘AWS ER70S-6’ 1.2 mm diameter which is specifically used for welding low carbon steel. The welding machine set up is shown in Fig. (1) together with the specimens before and after welding process.

2.4 Measurements of Joint Geometry Dimensions

After each welding test, the weldment were cut, sectioned, ground, polished and finally etched to see the profile of the joint geometry with necessary dimensions for measuring purpose, which is schematically similar to that was shown in reference ⁽¹³⁾, see Fig. (2). The weld joint geometry dimensions in terms of bead width, reinforcement height and bead penetration were measured after sectioning all specimens by using a digital caliper with accuracy ± 0.01 mm. The results of measurements for these three dimensions as responses are also listed in Table (4).

Since the heat input parameter has a significant effect on the quality of the joint geometry, therefore it was decided to calculate the values of heat input for all weldments by using the following equation ⁽⁴⁾:

$$Q = \frac{\eta * V * I * 60}{S * 1000} \dots\dots\dots (1)$$

Where, Q = Heat input (kJ/mm), V = Voltage (volt), I = Current (Amp.) S = Welding speed (mm/min) and η = Thermal efficiency.

For modeling and optimization the heat input at the same levels of used voltage, wire feed speed and gas flow rate, the current reading was taken during the welding process from the machine. Also, the welding speed was calculated for each test. Therefore, the heat input value was calculated for each welding test taking into account that the thermal efficiency is equal to 0.8 for MAG welding type ⁽⁵⁾. The results of calculated welding speed and heat input are listed in Table (5).

3. RESULTS & DISCUSSION

The response surface methodology was achieved using the Design of Expert version 8 software to determine the predicted models for the dimensions of the weld joint geometry (bead width, reinforcement height and depth of penetration), as responses in terms of the selected input parameters (arc voltage, wire feeding speed and gas flow rate). The analyses of variance (ANOVA) for RSM reduced quadratic models were determined for the bead dimensions as given in Tables (6, 7, and 8). The results in these tables showed that the voltage (A) and wire feeding speed (B) are statistically significant, since their P-values were

very small (< 0.5). This means that these two parameters contributed the highest effect on the weld joint geometry, while the gas flow rate has no influence on the bead width and reinforcement height [Tables (6 and 7)], since the gas flow rate term (C) is not in the model, except that it affects the penetration depth due to the appearance of this term in the model, as shown in Table (8).

The ANOVA analyses also pointed out that the quadratic effect was useful to incorporate into bead width and reinforcement models, since the second order terms were highly significant with a P-value lower than 0.05. In addition, it was noticed in Table (8) that the interaction (AB) of voltage and wire feeding speed and the interaction (BC) of wire speed rate and gas flow rate have the greatest impact on the weld penetration. Moreover, because the lack of fit was insignificant (P-value > 0.05) in Tables (6, 7 and 8), these three models are adequate and significant at 95% confidence. So, the final predicted equations for the weld geometry dimensions in terms of the actual input factors are:

$$\text{Bead width} = - 447.67946 + 41.63455 * \text{Voltage} + 0.36693 * \text{Wire feeding speed} - 1.01179 * \text{Voltage}^2 - 1.07286\text{E-}003 * \text{Wire feeding speed}^2 \dots\dots (2)$$

$$\text{Bead reinforcement height} = + 117.50250 - 9.62500 * \text{Voltage} - 0.19505 * \text{Wire feeding speed} + 5.70000\text{E-}003 * \text{Voltage} * \text{Wire feeding speed} + 0.21063 * \text{Voltage}^2 + 2.63000\text{E-}004 * \text{Wire feeding speed}^2 \dots\dots\dots (3)$$

$$\text{Bead Penetration} = + 17.22963 - 1.56938 * \text{Voltage} - 0.081675 * \text{Wire feeding speed} + 1.49031 * \text{Gas flow rate} + 9.85000\text{E-}003 * \text{Voltage} * \text{Wire feeding speed} - 0.010525 * \text{Wire feeding speed} * \text{Gas flow rate} \dots\dots\dots (4)$$

After the models were established, checking the adequacy of each model was conducted to examine the predicted model. Two types of model diagnostics, the normal probability plot and residuals versus the actual values plot, were used for verification, as shown in Figs. (3 and 4) for bead width. It can be seen from these plots that there was no violation of the normality assumption, since the normal probability plot followed a straight line pattern, the residual was normally distributed, and as long as the residual versus the predicted values show no unusual pattern and no outliers. Similar trends were observed in the plots related to the reinforcement and penetration models. Also, these three models showed a good agreement between the predicted and actual values for bead width, reinforcement height and penetration, as depicted in Fig. (5).

In order to see all input factors on one plot to provide silhouette views of the response surfaces, it helps to view the perturbation of the predicted responses caused by changing only one factor at a time from the center point of the experimental region. In other words, for response surface designs, the perturbation plot shows how the response changes as each

factor moves from the chosen reference point (at the middle of the design space), with all other factors held constant at the reference value. Accordingly, the perturbation plots for these three models are illustrated in Fig. (6). So, this figure indicates that, individually, both voltage and wire feeding speed largely affect the bead width and reinforcement, but they have a slight influence on the penetration. This is likely due to the higher heat input that increased the fusion of the material at the top surface of the joint. While, the gas flow rate has no effect on the bead width and reinforcement but slightly affect the penetration and this is may be due to the chemical affinity of the CO₂ gas with the molten material of the joint.

Since the diagnosis of the residuals reveals no statistical problems with the models, so the design of experiment generates the response surface plots in form of 2D contour, 3D surface and cube plots. Figures (7 and 8) show the 2D contour plots for the bead width and reinforcement, respectively as a function of voltage and wire feeding speed at gas flow rate of 10 L/min. It was found that welding at a gas flow rate of 8 and 12 L/min had no effect on these responses. It can be noticed from Fig.(7) that increasing both voltage and wire feeding speed increases the bead width due to the increase of quantity of the molten material that resulted by the increasing of the thermal input. Also, Fig. (8) shows that the increase of both voltage and wire speed decreases the reinforcement height, and this could be due to the higher fluidity effect of the molten material with increasing heat input.

Regarding the penetration model, Fig. (9) manifests the 3D surface plot for the weld penetration as a function of voltage and wire feeding speed at different gas flow rates. This figure depicts that all input parameters are effective in this model and have a slight increase on the bead penetration. However, the CO₂ gas is more effective than the other parameters at gas flow rate 8 L/min, Fig. (9a) due to the occurrence of higher penetration. And, this is attributed to the less chemical reaction of this gas with the molten material of the joint at this lower flow rate. Eventually, these observations are confirmed by the cube plot for penetration, as shown in Fig. (9d).

3.2 Modeling of Heat Input

Similarly for the heat input, the analysis of variance (ANOVA) for response quadratic model was constructed by DOE software as given in Table (9). This table shows that the input parameters as individual in addition to the quadratic terms of wire feeding speed and gas flow rate are all statistically significant and have the greatest influence on the heat input response according to their P-values (< 0.05). The lack of fit test indicates a good model, since it is insignificant with P-value greater than 0.05. So, this analysis indicates that this model is significant at 95% confidence. Also, this model showed a good agreement between

the predicted and actual values for heat input, as depicted in Fig. (10). so, the final predicted equation for the heat input in terms of the actual input factors is:

$$\text{Heat input} = - 7.06339 - 0.090188 * \text{Voltage} + 0.080047 * \text{Wire feeding speed} + 0.74389 * \text{Gas flow rate} - 2.42014\text{E-}004 * \text{Wire feeding speed}^2 - 0.039065 * \text{Gas flow rate}^2 \dots (5)$$

In order to diagnose the statistical properties of this model, it was found that the residuals that falling on a straight line implying errors are normally distributed. Also, the residuals versus predicted actual for heat input data exhibited no obvious pattern or unusual structure implying models are accurate.

To gain perspective on the model, it is necessary to present the perturbation of the predicted response resulted by varying only one parameter at a time from the center point of the investigated region. Fig. (11) demonstrates the perturbation plot for the heat input model, indicating that, individually, all input parameters affect the heat input response. The wire feeding speed largely increased the heat input because of more molten material accumulated in the weld joint at higher feeding speed, whereas both voltage and gas flow rate slightly reduced the heat input due to the higher wire speed and higher and more chemical reaction of CO₂ gas with the higher accumulated molten metal at the weld joint.

Because the diagnosis of the residuals manifested no statistical problems, the response surface plots were generated in terms of 3D surface plot, since all input parameters are significant in this model. Fig. (12) Depicts the 3D surface plot for the heat input response as a function of voltage and wire feeding speed at various gas flow rates. This figure shows the wire feeding speed is more effective on the heat input response at 10 L/min gas flow rate [Fig. (12b)] because of the higher molten material accumulated in the weld joint at higher feeding speed. Whereas both voltage and gas flow rate have a slight influence on heat input, and this is possibly ascribed to the higher wire speed and more chemical reaction of CO₂ with the more accumulated molten material in the weld joint. Finally, these observations are confirmed by the cube plot for penetration, as shown in Fig. (12d) for the heat input response.

3.3 Computational Optimization

A computational optimization method was used in this work by selecting the desired goals for each factor and response. This computational optimization is provided by the Design of Experiment software to find out the optimum combinations of parameters in order to fulfill the requirements as desired. Therefore, this software used for the optimization purpose; based on the data from the predictive models for four responses, weld bead width, reinforcement height, penetration and heat input as a function of three factors: arc voltage, wire feeding speed and gas flow rate.

The computational optimization process involves combining the goals into an overall desirability function. To develop the new predicted models, a new objective function, named 'Desirability' which allows to properly combining all the goals, was evaluated. Desirability is an objective function, to be maximized through a computational optimization, which ranges from zero to one at the goal. A higher value for desirability indicates the response value is more desirable. If it is equal to zero, this means a completely undesired response ⁽¹⁴⁾. Adjusting its weight or importance may alter the characteristics of a goal, and the aim of the optimization is to find a good set of conditions that will meet all the goals. Usually, the weights are used to establish an evaluation of the goal's importance when maximizing desirability function; in this work, weights are not changed since the four responses have the same importance and are not in conflict within each other.

The ultimate goal of this optimization was to obtain the maximum response that simultaneously satisfied all the variable properties. Table (10) lists the constraints of each variable for computational optimization of the weld bead width, reinforcement height, penetration and heat input. According to this table, five possible runs fulfilled this specified constraints to obtain the optimum values for weld bead width, reinforcement, penetration, heat input and desirability, as given in **Table (11)**. It can be seen that these runs gave a desirability of 0.686 with the optimum values of the weld bead width (9.4793 mm), reinforcement height(3.53625 mm), penetration (3.03997 mm), and heat input (1.27885 KJ/mm). Fig. (13) shows the 3D surface plot for desirability as a function of voltage and wire feeding speed at 8 L/min gas flow rate.

4. CONCLUSIONS

1. RSM achieved by DOE technique has shown its effectiveness and usefulness as a tool to predict the responses in MAG-CO₂ welding technique for any given input parameters.
2. Quadratic models were obtained by RSM achieved by DOE technique for the optimum heat input with the optimum dimensions of the weld joint geometry of the welded parts by the CO₂-MAG process.
3. The arc voltage and wire feeding speed are found the most effective welding parameters in the predicted quadratic models of weld bead width and reinforcement height, while gas flow rate is only influential in the predicted models of bead penetration and heat input.
4. Wire feeding speed is the most effective welding parameter in predicted quadratic model of the heat input, whereas both voltage and gas flow rate are less influential on this response.
5. Efficient weld joints could be achieved using the welding conditions drawn from the computational optimization. The optimum values of the weld bead width, reinforcement

height, penetration and heat input are (9.4793 mm), (3.53625 mm), (3.03997 mm), (1.27885 kJ/mm), respectively with a desirability of 0.686.

6. The results indicated that the process input parameters influence the heat input and the weld bead joint geometry to a significant extent.

ACKNOWLEDGEMENTS

The authors would like to acknowledge the technical support provided by the Korea-Iraq Vocational Training Center in Baghdad for achieving this research work. All technical facilities and kind assistance from Engineer Aziz Ibriheem Khlil (the general director of this center), Mr Firas Mohammed and Oday Aboud are gratefully acknowledged.

REFERENCES

1. 1.Biswajit Das, B. Debbarma, R. N. Rai and S. C. Saha, (2013), "Influence of Process Parameters on Depth of Penetration of Welded Joint in MIG Welding Process", International Journal of Research in Engineering and Technology (IJRET), Vol. 2, pp. 220-224.
2. Digvijay V. Jadeja and Satyam P. Patel, (2013), "A Review on Parametric Optimization by Factorial Design Approach of MAG-CO₂ Welding Process", International Journal of Engineering Research and Applications (IJERA), Vol. 3, Issue 2, pp. 420-424.
3. Praxair's International Locations, (1998), at: www.praxair.com, Inc. Praxair Technology.
4. O.P. Khanna, (2006), "A textbook of Welding Technology", Dhanpat Rai Publications Ltd.,pp.351.
5. Štefanija Klarić, Ivan Samardžić E. W. E, and Ivica Kladarić, (2008), "MAG Welding Process-Analysis of Welding Parameters Influence on Joint Geometry" '12th International Research/Expert Conference', Trends in the Development of Machinery and Associated Technology, TMT, Istanbul - Turkey, pp. 26-30.
6. S. C. Juang and Y. S. Tarng, (2002), "Process Parameters Selection for Optimizing the Weld Pool Geometry in the Tungsten Inert Gas Welding of Stainless Steel", Journal of Materials Processing Technology, Vol. 122, pp. 33-37.
7. D. S. Nagesh and G. L. Datta, (2002), "Prediction of Weld Bead Geometry and Penetration in Shielded Metal-arc Welding Using Artificial Neural Networks", Journal of Materials Processing Technology, Vol. 123, pp.303-312.
8. V. Gunaraj and N. Murugan, (1999), "Application of Response Surface Methodology for Predicting Weld Bead Quality in Submerged Arc Welding of Pipes", Journal of Materials Processing Tech., Vol. 88, pp. 266-275.

9. Biswajit Das, B. Debbarma, R. N. Rai and S. C. Saha, (2013), "Influence of Process Parameters on Depth of Penetration of Welded Joint in MIG Welding Process" International Journal of Research in Engineering and Technology, Volume: 02, pp. 220-224.
10. Mohd. Shoeb, Mohd. Parvez and Pratibha Kumari, (2013), "Effect of MIG Welding Input Process Parameters on Weld Bead Geometry on HSLA Steel" International Journal of Engineering Science and Technology (IJEST), Vol. 5 No.01, pp. 200 – 212.
11. Parth D Patel, Sachin P Patel, (2011), "Prediction of Weld Strength of Metal Active Gas (MAG) Welding Using Artificial Neural Network", International Journal of Engineering Research and Applications (IJERA), Vol. 1, pp. 36 - 44.
12. Thomas G. Digges and Samuel J. Rosenberg, (1960), "Heat Transfer and Properties of Iron and Steel", National Bureau of Standards Monograph 18.
13. Vinod Kumar, (2010), "Development and Characterization of Fluxes for Submerged Arc Welding" A thesis Doctor of Philosophy in Mechanical Engineering, College of Engineering – Punjabi University, Patiala-Indian.
14. R. H. MYERS and D. C. Montgomery, (1995), "Response Surface Methodology- Process and Product Optimization Using Designed Experiment", John Wiley & Sons.

Table (1): Chemical Composition for Used LCS with Standard Type (wt%).

Material	C	Si	Mn	P	S	Cr	Mo	Ni	Al	Co	Cu	V	Fe
Experimental	0.13	0.015	0.450	0.003	0.003	0.001	0.002	0.043	0.036	0.007	0.001	0.001	Bal.
Standard Steel AISI 101 (12)	0.08 – 0.13	0.1 max	0.3 – 0.6	0.04 max	0.05 max	--	--	--	--	--	--	--	Bal.

Table (2): Mechanical Properties for Used LCS with Standard Type (wt%).

Material	Yield strength (MPa)	Tensile strength (MPa)	Elongation (%)
Experimental	262	391	42

Table (3): Levels of input parameters used with respective coding.

+alpha	-alpha	High Level + 1	Low Level - 1	Unit	Input parameter
22	18	21	19	Volt	Voltage
200	100	175	125	cm/min	Wire feeding speed
14	5	12	8	L/min	Gas flow rate

Table (4): Design Matrix for Input Factors and Experimental Values of Output (Responses).

Bead penetration (mm)	Bead reinforcement (mm)	Bead width (mm)	Gas flow rate (L/min)	Wire feed speed (cm/min)	Voltage (volt)	Type of point	Run No.	Std
1.93	3.87	7.18	8	125	19	Factorial	12	1
1.4	3	9.52	8	125	21	Factorial	7	2
3.04	3.68	9.17	8	175	19	Factorial	8	3
3.34	3.04	10.82	8	175	21	Factorial	1	4
2.76	3.98	7.13	12	125	19	Factorial	14	5
2	2.82	8.75	12	125	21	Factorial	4	6
1.61	3.5	8.98	12	175	19	Factorial	16	7
1.99	3.25	12.58	12	175	21	Factorial	18	8
2.43	4.5	5.05	10	150	18	Axial	9	9
2	3.2	9.75	10	150	22	Axial	15	10
1.68	3.83	6.5	10	100	20	Axial	6	11
2.75	3.5	11.03	10	200	20	Axial	2	12
2.62	3.03	11.78	6	150	20	Axial	19	13
1.88	2.97	11.03	14	150	20	Axial	10	14
2.42	3.17	12	10	150	20	Center	3	15
2.32	3.04	11.5	10	150	20	Center	11	16
2.2	3.02	11.24	10	150	20	Center	17	17
2.3	3	10.81	10	150	20	Center	5	18
2.12	2.85	11.51	10	150	20	Center	13	19
2.34	3	10.71	10	150	20	Center	20	20

Table (5): The Results of Calculated Welding Speed and Heat Input.

Calculated Heat input (KJ/mm)	Calculated Welding Speed (mm/min)	Welding Current (Amp.)	Welding Voltage (volt)	Type of point	Run No.	Std
0.85	64.6	60	19	Factorial	12	1
0.7	73.1	51	21	Factorial	7	2
1.31	90	129	19	Factorial	8	3
1	105	104	21	Factorial	1	4
0.74	69.7	57	19	Factorial	14	5
0.55	85.7	47	21	Factorial	4	6
1.1	103.4	125	19	Factorial	16	7
0.96	115.4	110	21	Factorial	18	8
1.4	66.7	108	18	Axial	9	9
1.08	85	87	22	Axial	15	10
0.28	65	19	20	Axial	6	11
1	125	130	20	Axial	2	12
0.79	95.32	78	20	Axial	19	13
0.45	115	54	20	Axial	10	14
1.2	70	87	20	Center	3	15
1.25	76.92	100	20	Center	11	16
1.31	74.5	102	20	Center	17	17
1.3	71	96	20	Center	5	18
1.15	76.5	92	20	Center	13	19
1.19	72.8	90	20	Center	20	20

Table (6): Analysis of Variance (ANOVA) for Response Surface Reduced Quadratic Model (Bead width).

p-value Prob > F	F value	Mean square	df	Sum of squares	Source
< 0.0001 significant	64.21	18.88	4	75.52	Model
<0.0001	73.62	21.65	1	21.65	A-Voltage
<0.0001	69.10	20.32	1	20.32	B-Wire feeding speed
< 0.0001	91.75	26.98	1	26.98	A ²
< 0.0001	40.30	11.85	1	11.85	B ²
		0.29	15	4.41	Residual
0.3758 not significant	1.39	0.32	10	3.24	Lack of Fit
		0.23	5	1.17	Purr Error
			19	79.94	Core Total
R-Squared = 0.9448			Std. Dev. = 0.54		
Adj R-Squared = 0.9301			Mean = 9.85		
Pred R-Squared = 0.8971			C.V. % = 5.50		
Adeq Precision = 25.749			PRESS = 8.22		

Table (7): Analysis of Variance (ANOVA) for Response Surface Reduced Quadratic Model (Bead Rienforcement).

p-value Prob > F	F value	Mean square	Df	Sum of squares	Source
< 0.0001 significant	77.27	0.74	5	3.72	Model
<0.0001	197.68	1.90	1	1.90	A-Voltage
<0.0459	4.80	0.046	1	0.046	B-Wire feeding speed
0.0011	16.86	0.16	1	0.16	AB
< 0.0001	121.35	1.17	1	1.17	A ²
< 0.0001	73.91	0.71	1	0.71	B ²
		9.634E-003	14	0.13	Residual
0.5944 not significant	0.88	9.171E-003	9	0.083	Lack of Fit
		0.010	5	0.052	Purr Error
			19	3.86	Core Total
R-Squared = 0.9650			Std. Dev. = 0.098		
Adj R-Squared = 0.9525			Mean = 3.31		
Pred R-Squared = 0.9197			C.V. % = 2.96		
Adeq Precision = 29.599			PRESS = 0.31		

Table (8): Analysis of Variance (ANOVA) for Response Surface Reduced Quadratic Model (Bead Penetration).

p-value Prob > F	F value	Mean square	Df	Sum of squares	Source
< 0.0001 significant	132.20	0.87	5	4.35	Model
0.0005	20.52	0.14	1	0.14	A-Voltage
<0.0001	154.19	1.02	1	1.02	B-Wire feeding speed
< 0.0001	76.04	0.50	1	0.50	C-Gas flow rate
< 0.0001	73.69	0.49	1	0.49	AB
< 0.0001	336.55	2.22	1	2.22	BC
		6.583E-003	14	0.092	Residual
0.9237 not significant	0.34	3.892E-003	9	0.035	Lack of Fit
		0.011	5	0.057	Purr Error
			19	4.44	Core Total
R-Squared = 0.9793			Std. Dev. = 0.081		
Adj R-Squared = 0.9719			Mean = 2.26		
Pred R-Squared = 0.9629			C.V. % = 3.60		
Adeq Precision = 42.102			PRESS = 0.16		

Table (9): Analysis of Variance (ANOVA) for Response Surface Reduced Quadratic Model (Heat Input).

p-value Prob > F	F value	Mean square	Df	Sum of squares	Source
< 0.0001 significant	134.09	0.37	5	1.83	Model
< 0.0001	47.60	0.13	1	0.13	A-Voltage
<0.0001	202.59	0.55	1	0.55	B-Wire feeding speed
< 0.0001	32.75	0.090	1	0.090	C-Gas flow rate
< 0.0001	220.52	0.60	1	0.60	B ²
< 0.0001	235.34	0.64	1	0.64	C ²
		2.734E-003	14	0.038	Residual
0.8401 not significant	0.48	1.972E-003	9	0.018	Lack of Fit
		4.107E-003	5	0.021	Purr Error
			19	1.87	Core Total
R-Squared = 0.9795				Std. Dev. = 0.052	
Adj R-Squared = 0.9722				Mean = 0.98	
Pred R-Squared = 0.9591				C.V. % = 5.33	
Adeq Precision = 40.417				PRESS = 0.077	

Table (10): Constrains Used for the Computational Optimization.

Importance	Upper Weight	Lower Weight	Upper Limit	Lower Limit	Goal	Name
3	1	1	21	19	is in range	A:Voltage
3	1	1	175	125	is in range	B:Wire feeding speed
3	1	1	12	8	is in range	C:Gas flow rate
3	1	1	12.58	5.05	maximize	Bead width
3	1	1	4.5	2.82	maximize	Bead reinforcement
3	1	1	3.34	1.4	maximize	Penetration
3	1	1	1.408	0.28	maximize	Heat input

Table (11): The Optimum Solutions of the Desirability.

Desirability	Heat input (KJ/mm)	Penetration (mm)	Bead reinforcement (mm)	Bead Width (mm)	Gas flow rate (L/min)	Wire feeding speed (mm/min)	Voltage (Volt)	No.
<u>0.686 selected</u>	<u>1.27885</u>	<u>3.03997</u>	<u>3.53625</u>	<u>9.4793</u>	8	175	19	1
0.686	1.28271	3.02974	3.53624	9.47931	8	175	19	2
0.686	1.28579	3.02143	3.53625	9.47929	8	175	19	3
0.686	1.27745	3.03992	3.52646	9.52929	8	175	19	4
0.686	1.27662	3.03999	3.53439	9.48221	8	175	19	5



Fig. (1): CO₂-MAG Welding Machine and Specimens Before and After Welding.

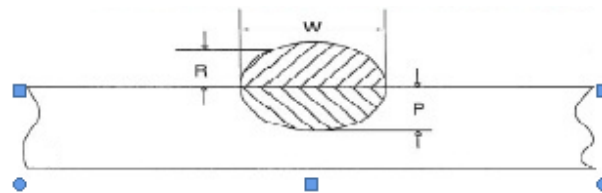


Fig. (2): A schematic Illustration Profile of the Joint Geometry ⁽¹³⁾.

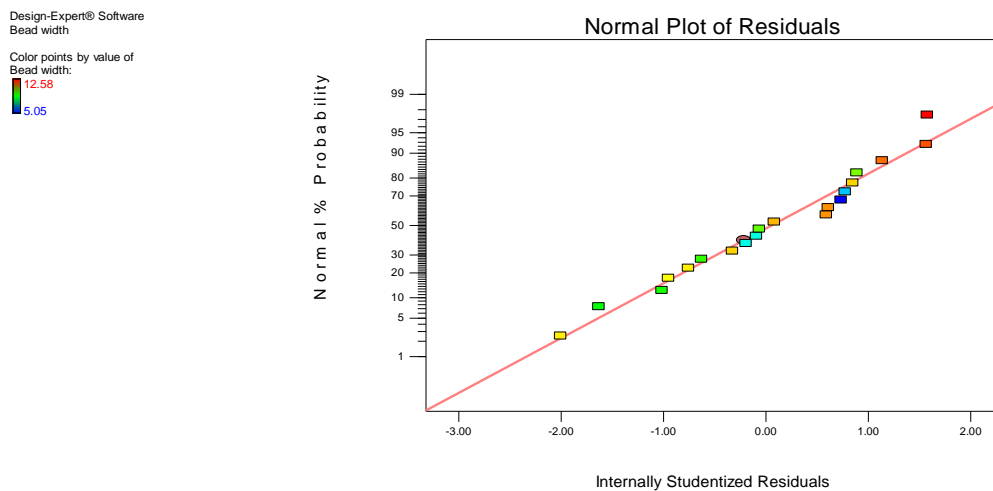


Fig. (3): Normal Probability Plot of Residuals for Bead Width Data.

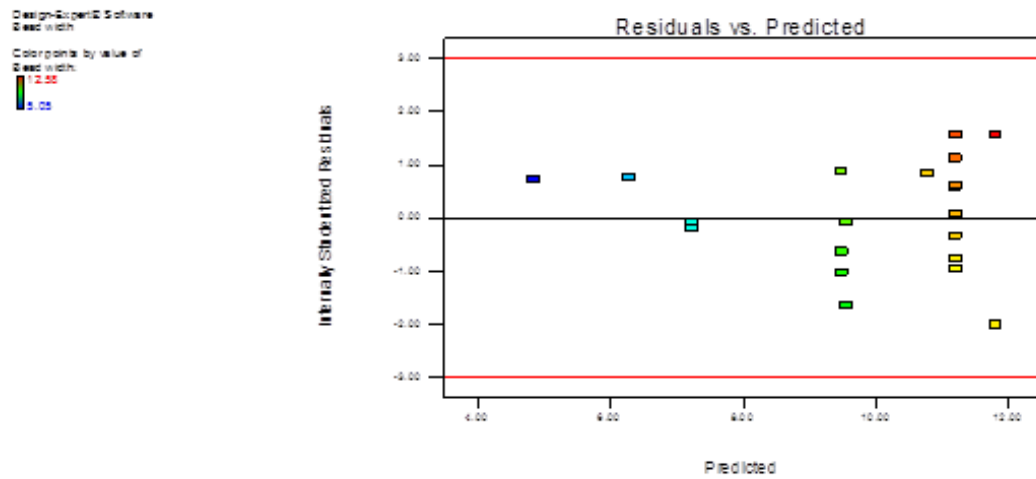
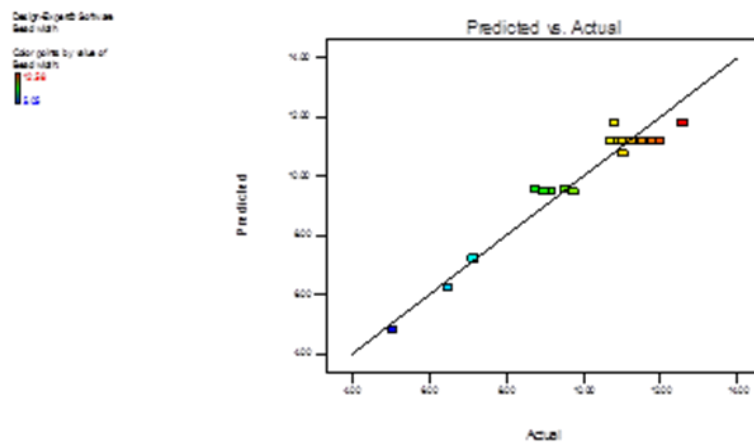
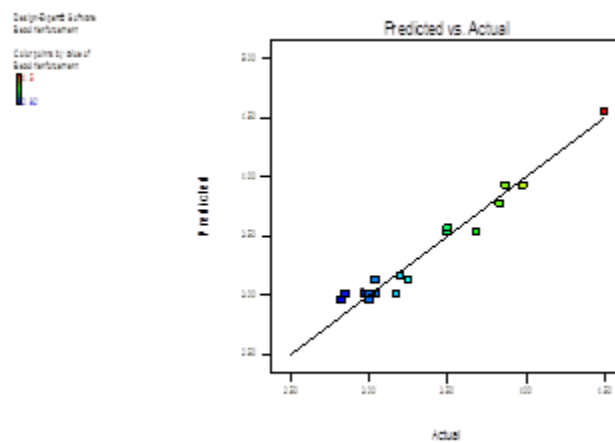


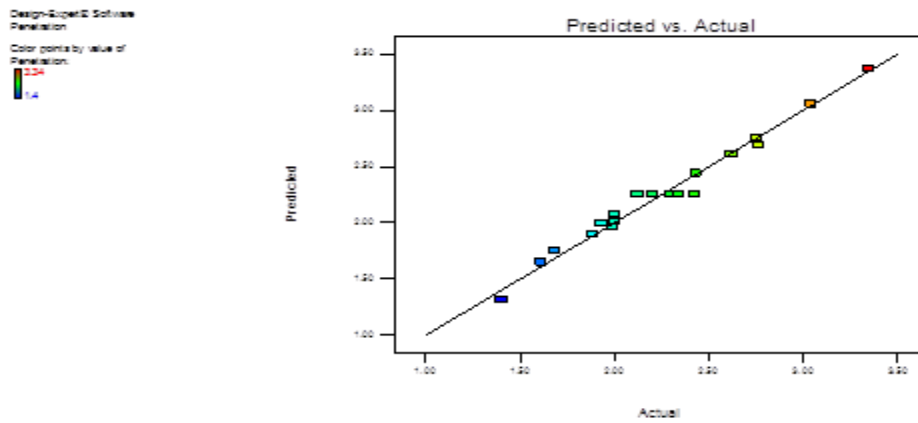
Fig. (4): Residual versus Predicted Responses for Bead Width Data.



(A)

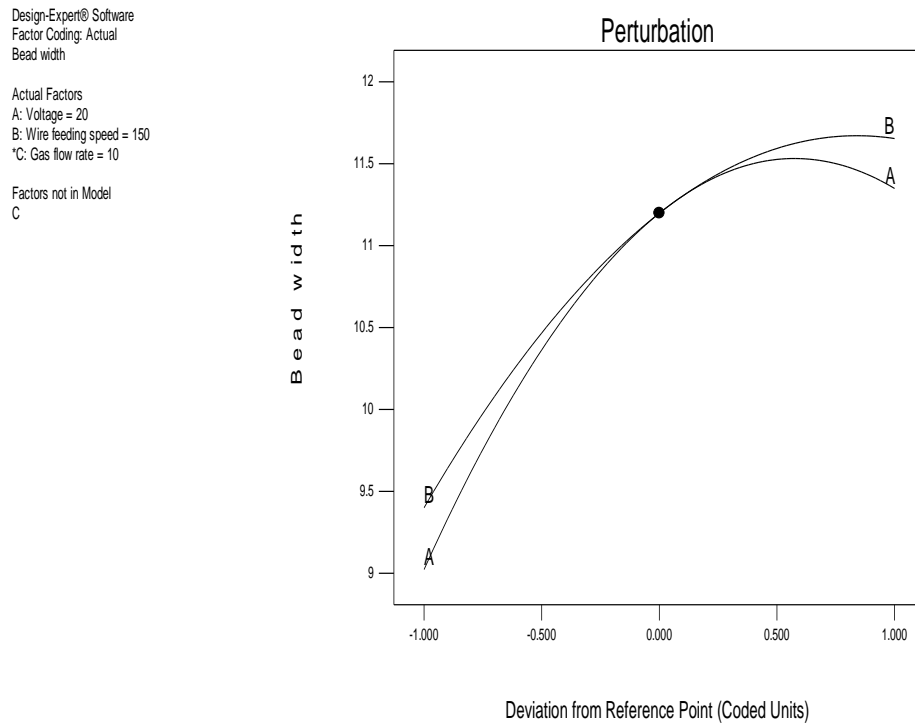


(B)



(C)

Fig. (5): Predicted versus actual for (A) bead width data, (B) reinforcement and (C) Penetration.

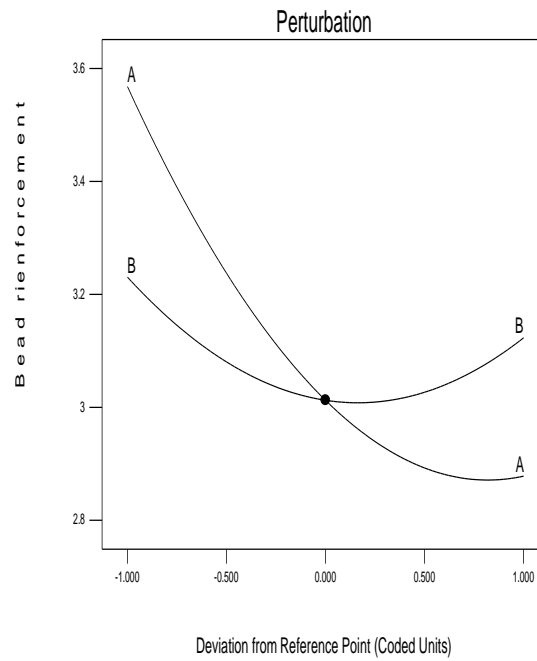


(A)

Design-Expert® Software
 Factor Coding: Actual
 Bead reinforcement

Actual Factors
 A: Voltage = 20
 B: Wire feeding speed = 150
 *C: Gas flow rate = 10

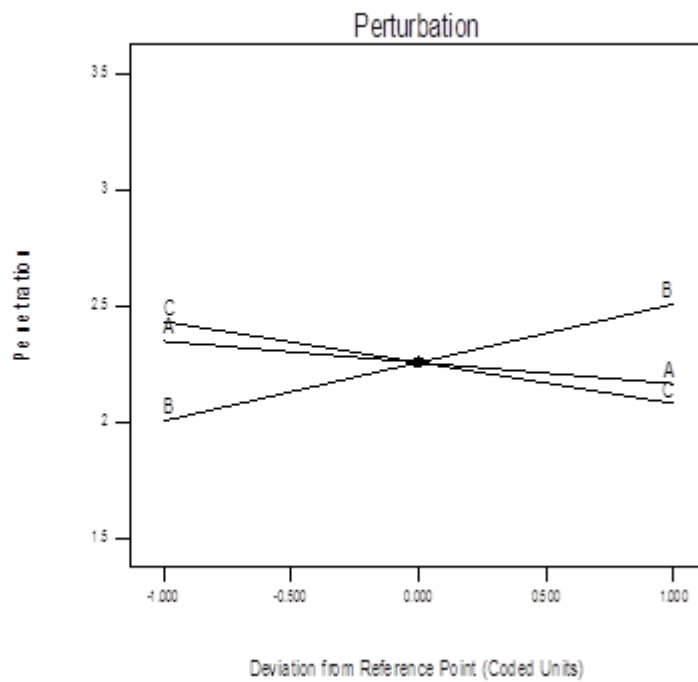
Factors not in Model
 C



(B)

Design-Expert® Software
 Factor Coding: Actual
 Penetration

Actual Factors
 A: Voltage = 20
 B: Wire feeding speed = 150
 C: Gas flow rate = 10



(C)

Fig. (6): Perturbation of (A) Bead Width, (B) Reinforcement and (C) Penetration on Wire Feeding Speed and Gas Flow Rate.

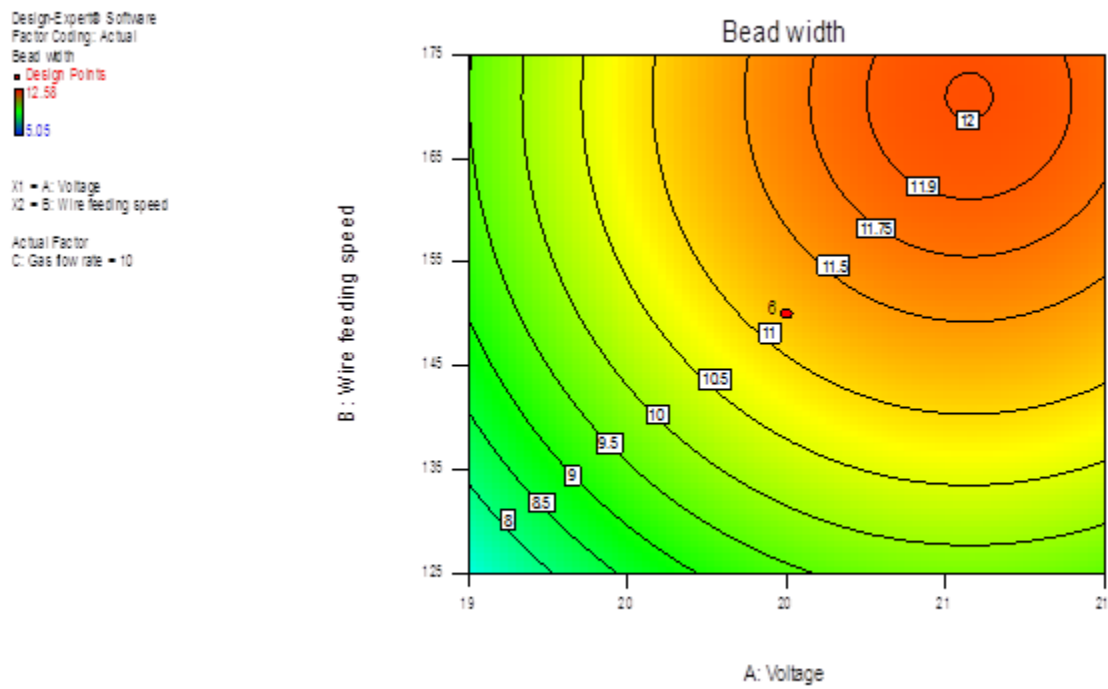


Fig. (7): Contour Graph of Bead Width as A functions of Voltage and Wire Feeding Speed at 10 L/min Gas Flow Rate.

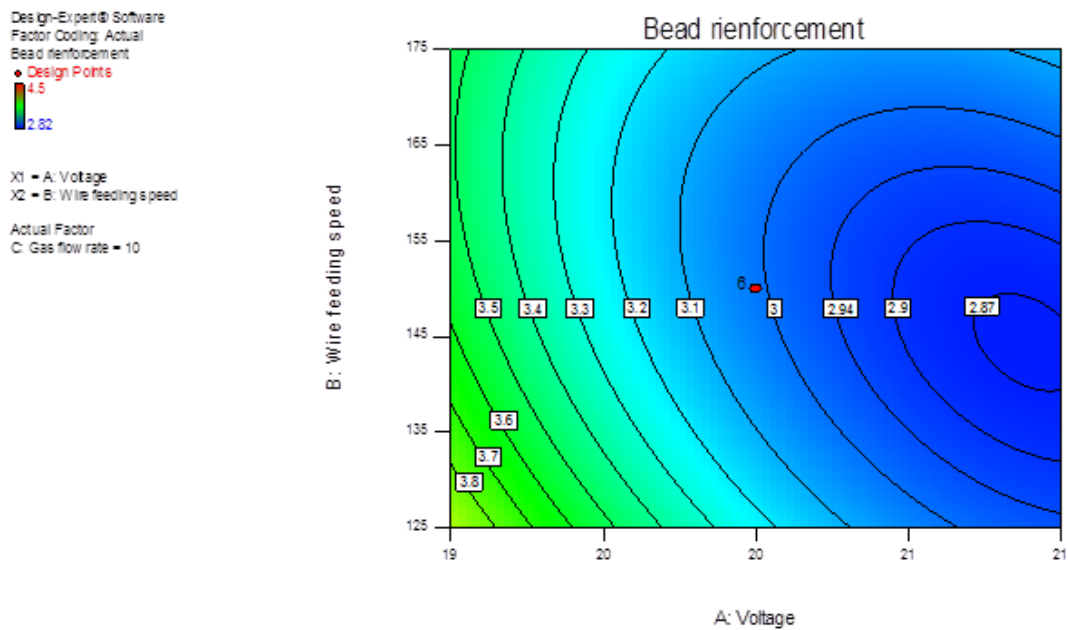
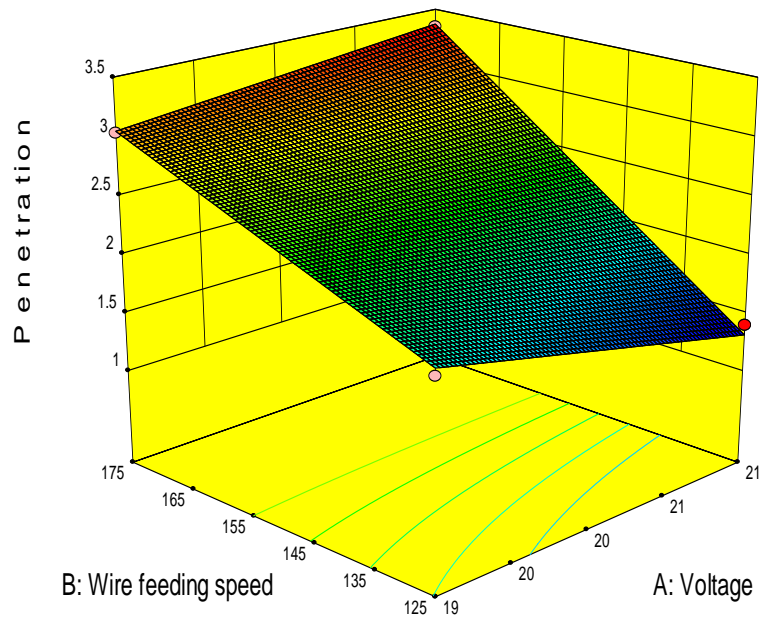


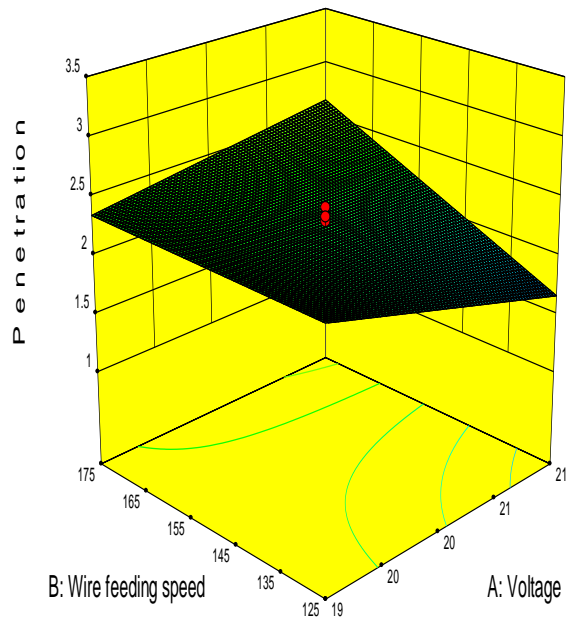
Fig. (8): Contour Graph of Bead Reinforcement as A functions of Voltage and Wire Feeding Speed at 10 L/min Gas Flow Rate.

Design-Expert® Software
 Factor Coding: Actual
 Penetration
 ● Design points above predicted value
 ○ Design points below predicted value
 3.34
 1.4
 X1 = A: Voltage
 X2 = B: Wire feeding speed
 Actual Factor
 C: Gas flow rate = 8



(A)

Design-Expert® Software
 Factor Coding: Actual
 Penetration
 ● Design points above predicted value
 ○ Design points below predicted value
 3.34
 1.4
 X1 = A: Voltage
 X2 = B: Wire feeding speed
 Actual Factor
 C: Gas flow rate = 10



(B)

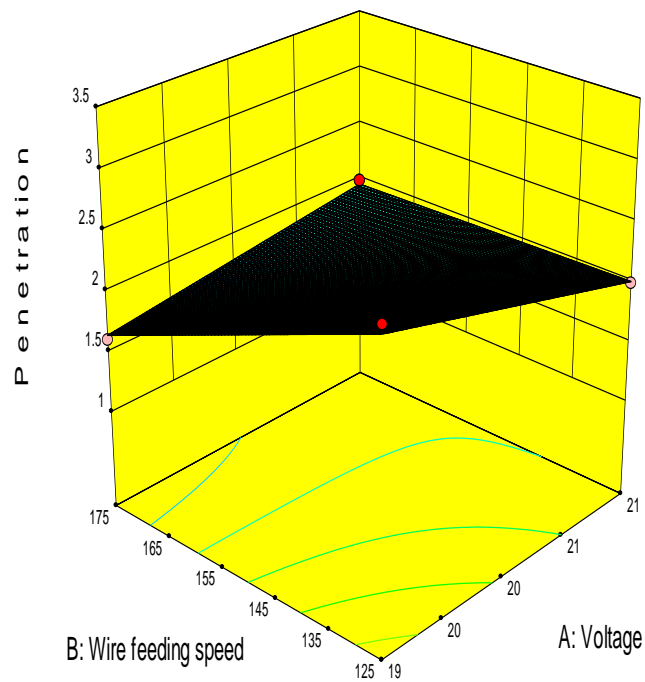
Design-Expert® Software
 Factor Coding: Actual
 Penetration

● Design points above predicted value
 ○ Design points below predicted value



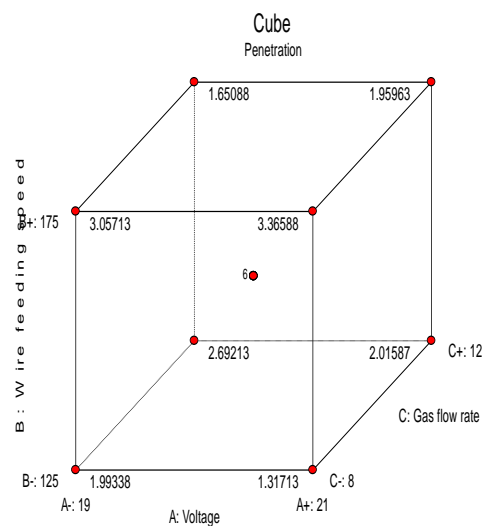
X1 = A: Voltage
 X2 = B: Wire feeding speed

Actual Factor
 C: Gas flow rate = 12



(C)

Design-Expert® Software
 Factor Coding: Actual
 Penetration
 X1 = A: Voltage
 X2 = B: Wire feeding speed
 X3 = C: Gas flow rate



(D)

Fig. (9): 3D Graph of Bead Penetration as A function of Voltage and Wire Feeding Speed at (A, B, C) Gas Flow Rate 8, 10 and 12 L/min, respectively and (D) Cube Shape for Penetration.

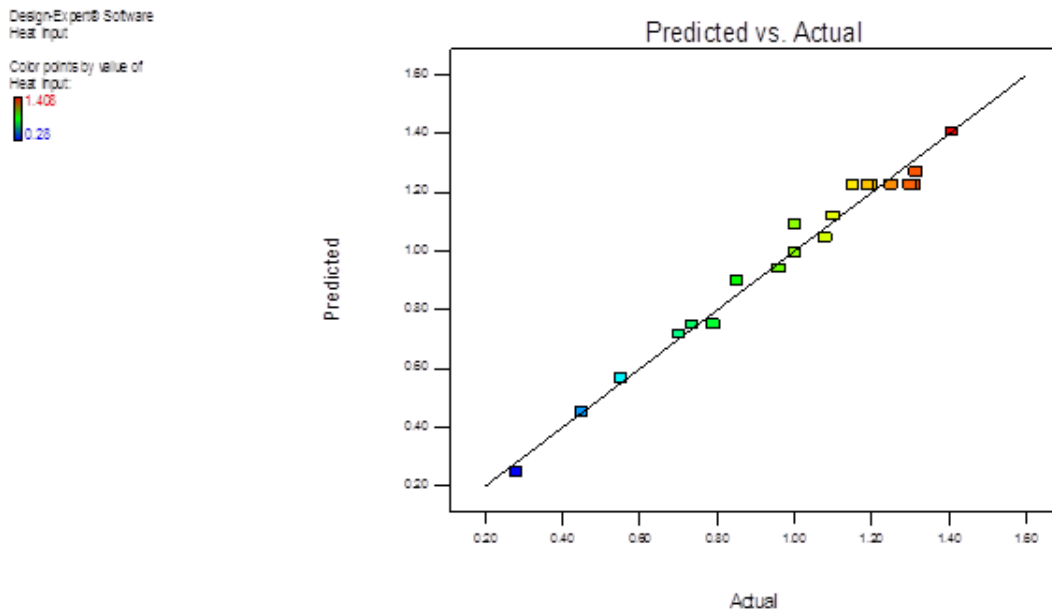


Fig. (10): Predicted Versus Actual Heat Input Data.

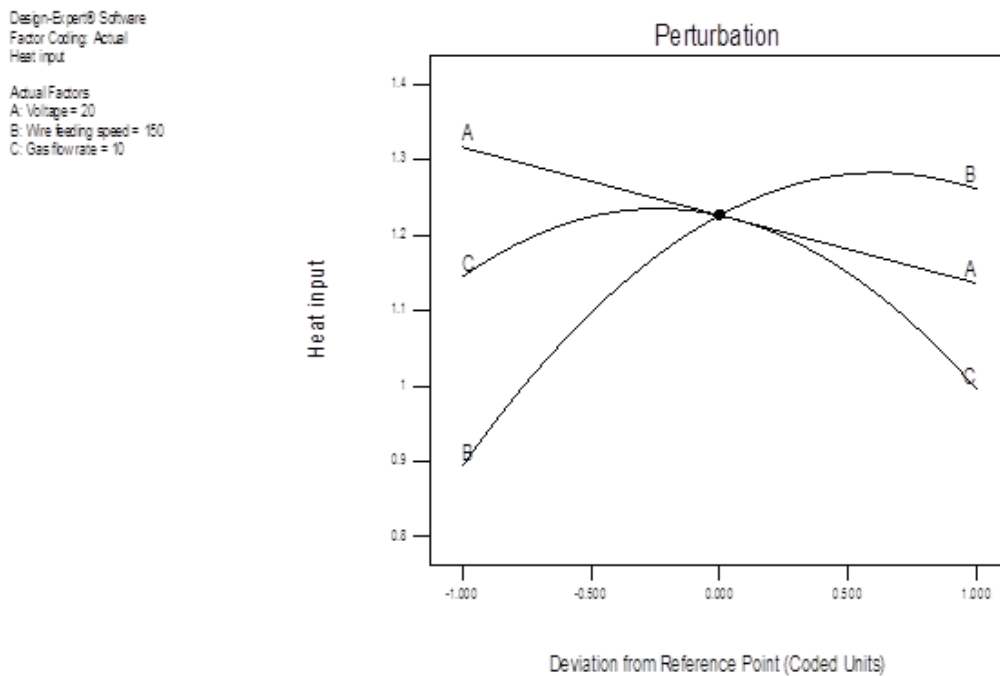
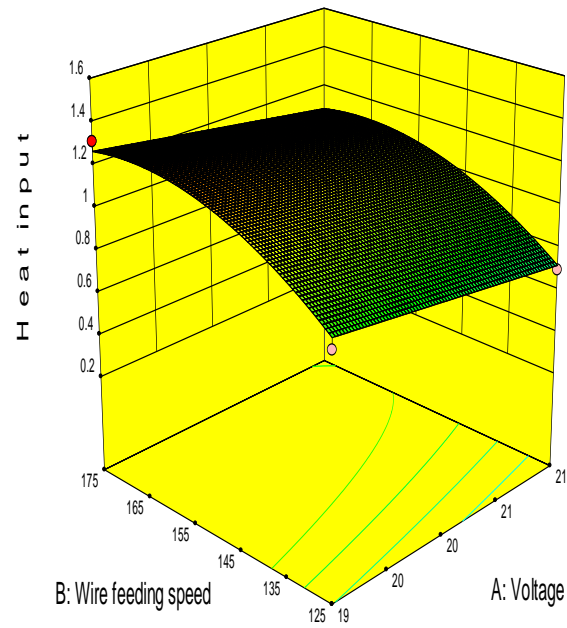


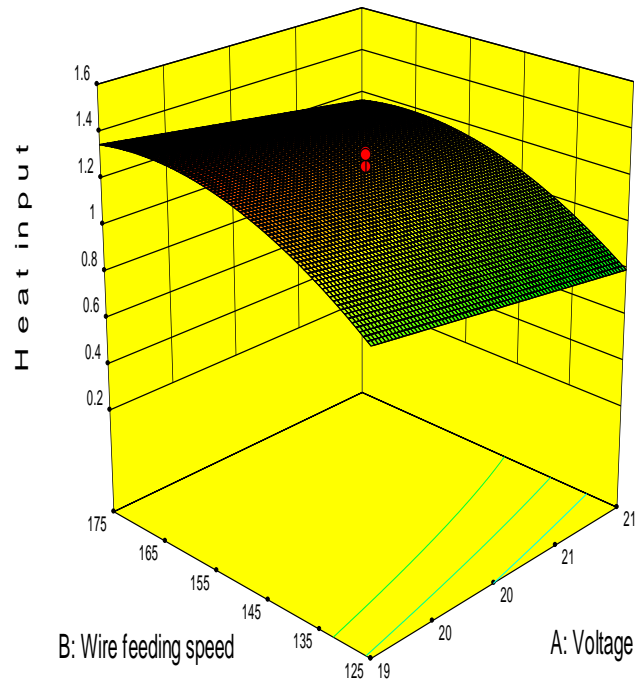
Fig. (11): Perturbation of Heat Input on Wire Feeding Speed and Gas Flow Rate.

Design-Expert® Software
 Factor Coding: Actual
 Heat input
 ● Design points above predicted value
 ○ Design points below predicted value
 1.408
 0.3
 X1 = A: Voltage
 X2 = B: Wire feeding speed
 Actual Factor
 C: Gas flow rate = 8



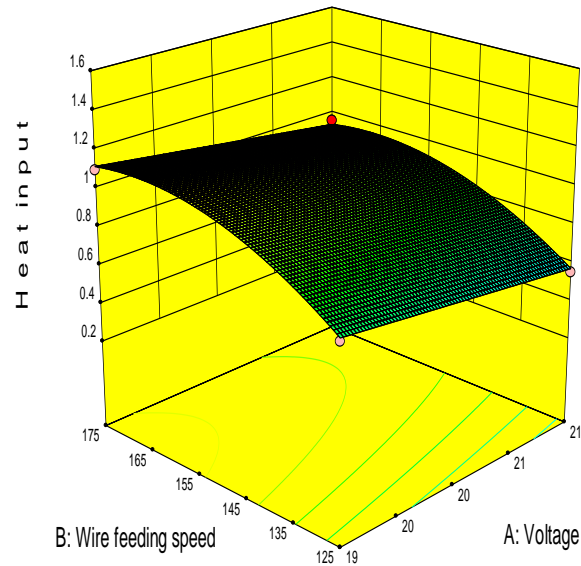
(A)

Design-Expert® Software
 Factor Coding: Actual
 Heat input
 ● Design points above predicted value
 ○ Design points below predicted value
 1.408
 0.3
 X1 = A: Voltage
 X2 = B: Wire feeding speed
 Actual Factor
 C: Gas flow rate = 10



(B)

Design-Expert® Software
 Factor Coding: Actual
 Heat input
 ● Design points above predicted value
 ○ Design points below predicted value
 1.408
 0.3
 X1 = A: Voltage
 X2 = B: Wire feeding speed
 Actual Factor
 C: Gas flow rate = 12



Design-Expert® Software
 Factor Coding: Actual
 Heat input
 X1 = A: Voltage
 X2 = B: Wire feeding speed
 X3 = C: Gas flow rate

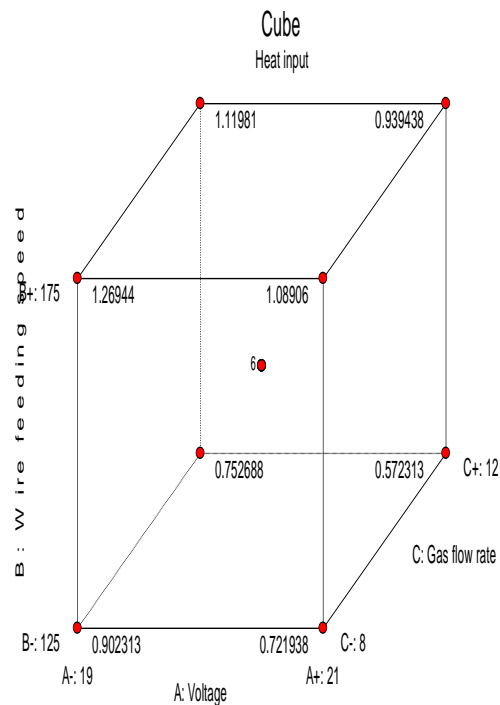


Fig. (12): 3D Graph of Heat Input as A function of Voltage and Wire Feeding Speed (A, B, C) at Gas Flow Rates 8, 10 and 12 L/min, respectively and (D) Cube Shape for Heat Input

Design-Expert® Software
Factor Coding: Actual
Desirability
1.000
0.000
X1 = A: Voltage
X2 = B: Wire feeding speed
Actual Factor
C: Gas flow rate = 8

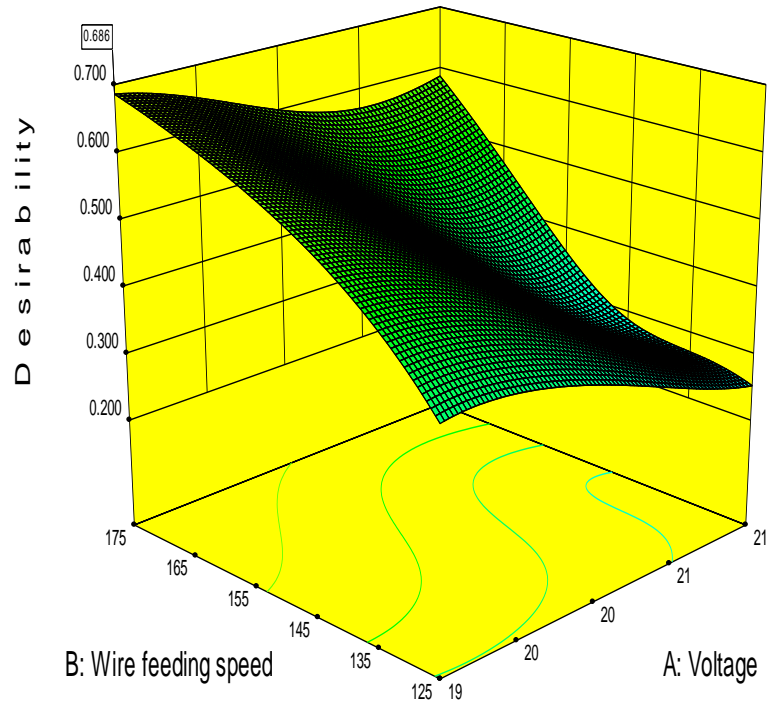


Fig. (13): 3D Surface Plot for Desirability.

دراسة تأثير عوامل عملية لحام القوس المعدني بغاز CO₂ على الحرارة الداخلة وأبعاد الشكل الهندسي لوصلة اللحام باستخدام الطرق المختبرية والحاسوبية

صلاح صبيح عبد الكريم
مدرس
جامعة بغداد- كلية الزراعة
قسم المكنات والآلات الزراعية

سمير علي أمين الربيعي
أستاذ مساعد
الجامعة التكنولوجية
قسم المكنات والمعدات

الخلاصة

في هذا البحث تم التنبؤ بموديل بالحرارة الداخلة وأبعاد الشكل الهندسي للوصلة الملحومة بطريقة لحام القوس المعدني بغاز ثاني أكسيد الكربون عن طريق عمل نماذج رياضية لهذا الغرض. قبل عملية اللحام تم تهيئة عينات الاختبار العملية للصلب و لحامها تناكبيا" بعد ذلك باستخدام سلك لحام منصهر في بركة اللحام بأدخال الحرارة الداخلة بشكل مستمر. تم قياس أبعاد درزة اللحام ومن ثم تحليل نتائجها للتحقق من صحة النماذج باستخدام تقنية تصميم التجارب وطريقة الاستجابة السطحية. هذه النماذج وجدت لتكون قادرة على التنبؤ بأمتلية الأبعاد المطلوبة للشكل الهندسي بدلالة عرض درزة اللحام، ارتفاع المنطقة المقواة باللحام وعمق اللحام. بينت النتائج المستحصلة بأن الحرارة الداخلة تعتمد على الفولتية، سرعة تغذية السلك ومعدل جريان الغاز بينما فيما يخص أبعاد درزة اللحام فان تأثير معدل جريان الغاز عليها كان قليل. تمت المقارنة بين النتائج العملية والنتائج الحاسوبية ووجد ان هناك تطابق جيد بينهما.